Journal of Medicinal Chemistry

Article

pubs.acs.org/jmc

Synthesis and Biological Evaluation of a New Series of Hexahydro-2*H*-pyrano[3,2-*c*]quinolines as Novel Selective σ_1 Receptor Ligands

José Luis Díaz,*[,†] Ute Christmann,[†] Ariadna Fernández,[†] Mónica Luengo,[†] Magda Bordas,[†] Raquel Enrech,[†] Mónica Carro,[†] Rosalia Pascual,[†] Javier Burgueño,[†] Manuel Merlos,[†] Jordi Benet-Buchholz,[‡] Jordi Cerón-Bertran,[‡] Jesús Ramírez,[‡] Raquel F. Reinoso,[†] Antonio R. Fernández de Henestrosa,[†] José Miguel Vela,[†] and Carmen Almansa*[,†]

[†]Drug Discovery and Preclinical Development, Esteve, Baldiri Reixach 4-8, 08028 Barcelona, Spain

[‡]Crysforma, Institute of Chemical Research of Catalonia (ICIQ), Avinguda Països Catalans 16, E-43007 Tarragona, Spain

Supporting Information

ABSTRACT: The synthesis and pharmacological activity of a new series of hexahydro-2*H*-pyrano[3,2-*c*]quinoline derivatives as potent σ_1 receptor (σ_1R) ligands are reported. This family, which does not contain the highly basic amino group usually present in other σ_1R ligands, showed high selectivity over the σ_2 receptor (σ_2R). The activity was shown to reside in only one of the four possible diastereoisomers, which exhibited a perfect match with known σ_1R pharmacophores. A hit to lead program based on a high-throughput screening hit (**8a**) led to the identification of compound **32c**, with substantially improved activity and physicochemical properties. Compound **32c** also exhibited a good ADMET (absorption, distribution, metabolism, excretion, toxicity) profile and was identified as a σ_1R antagonist on the basis of its analgesic activity in the mouse capsaicin and formalin models of neurogenic pain.

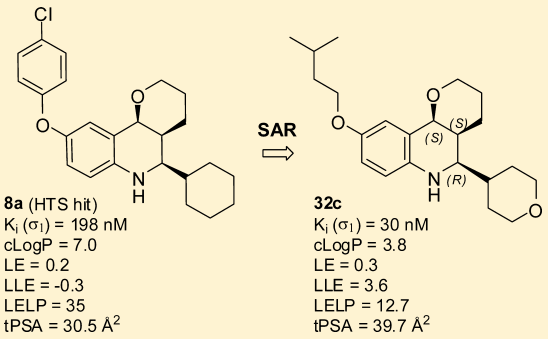

INTRODUCTION

The σ receptors were discovered in the mid-1970s and originally proposed as a new class of opioid receptors. At present it is known that σ receptors are unique binding sites with no homology to opioid receptors or other mammalian proteins. Pharmacological studies have identified at least two distinct subtypes, namely, σ_1 and σ_2.[1] The receptor (σ_1R) has been cloned and shown to encode a protein anchored to the endoplasmic reticulum and plasma membranes.[2] This protein acts as a unique ligand-regulated molecular chaperone[3] that modulates the activity of different proteins, such as *N*-methyl-D-aspartic (NMDA) receptors[4] and several ion channels.[5] Additionally, σ_1R has been known to modulate opioid analgesia,[6] and the relationship between the μ-opioid and σ_1 receptors has been recently shown to involve direct physical interaction,[7] which explains why σ_1R antagonists enhance the antinociceptive effect of opioids.

No selective σ_1R ligands have so far been marketed, but several nonselective compounds have been assayed in clinical studies as antidepressants, drug abuse treatments, antipsychotics, and learning and memory enhancers.[8] Our group became interested in the potential role of σ_1R in pain control, and a σ_1R knockout mouse was developed, showing attenuated pain responses in the formalin test[9] and no mechanical hypersensitivity following capsaicin sensitization[10] or sciatic nerve injury.[11] The key role played by σ_1R in pain-related central sensitization phenomena[11,12] and the effect shown by several of our σ_1R antagonists[13] in different models of nociceptive and neuropathic pain support the involvement of σ_1R in the control of nociception. Several compounds have been evaluated for the treatment of pain, and compound **1**,[14] which is currently in clinical trials for the treatment of diverse pain states, is the most advanced one. Compound **1** was developed on the basis of the pharmacophoric model described by Glennon et al.,[15] which involves a basic amino group and at least two hydrophobic regions at a certain distance from this basic amino group, a structural feature shared by other prototypical σ_1R antagonists,[16] such as BD-1063 (**2**) and haloperidol (**3**) (Figure 1A,B).

On the other hand, σ_2R still remains to be unambiguously identified, although progesterone receptor membrane component 1 (PGRMC1), a cytochrome-related protein that binds directly to heme and regulates lipid and drug metabolism and hormone signaling, has been recently proposed as the putative σ_2R binding site.[17] Ligands acting on σ_2R have been proposed as biomarkers for tumor cell proliferation and show pro-apoptotic properties, thus suggesting a potential role in cancer

Received: February 4, 2013
Published: April 8, 2013

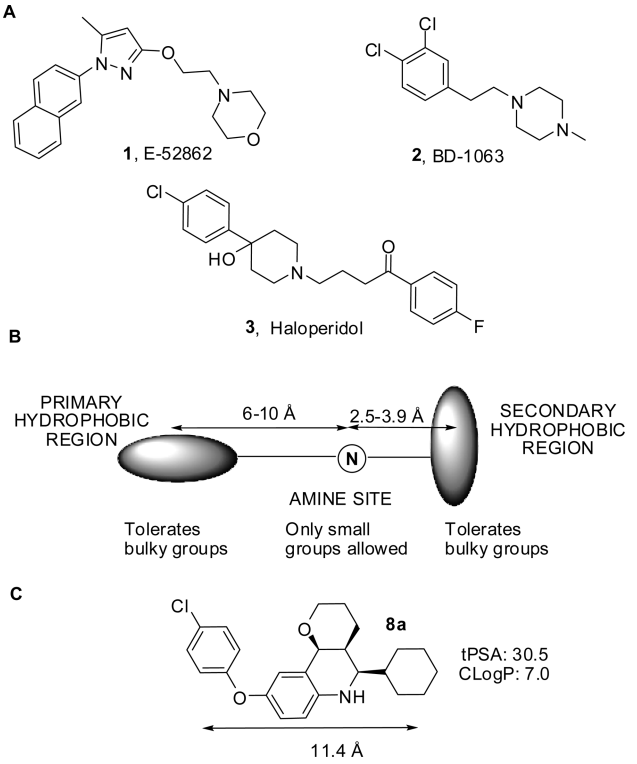

Figure 1. Representative σ_1R antagonists (A), pharmacophoric σ_1R model by Glennon (B),[25] and structure of the initial hit **8a** (C).

imaging and treatment.[18] Because the pharmacologies of the two σ receptors are clearly differentiated, selectivity between both of them and against other molecular targets is desired.

As a result of a high-throughput screening (HTS) program devoted to the discovery of new σ_1R antagonists, we identified a new series of hexahydro-2*H*-pyrano[3,2-*c*]quinolines which showed high selectivity over σ_2R but contained an aniline-like weak basic nitrogen, instead of the usual tertiary or secondary alkylamino group. We report herein the structure–activity relationship (SAR) studies that allowed the optimization of the activity and physicochemical properties of the initial hit **8a** (Figure 1C).

CHEMISTRY

The synthesis of the new furano- and pyranoquinolines was accomplished by the Povarov reaction,[19] which provided a "one-pot" ready access to the compounds. The multicomponent reaction of substituted anilines (**4**), aldehydes (**5**), and dihydrofuran (**6**) or dihydropyran (**7**) mediated by the Lewis catalyst $Mg(ClO_4)_2$[20] in acetonitrile provided the fused quinolines **8**–**33** (Scheme 1). Other Lewis catalysts such as I_2[21] or (TMS)Cl[22] were tested, but $Mg(ClO_4)_2$ gave the best results in terms of yields and purity, especially when aliphatic cyclic aldehydes were employed. As expected, in this formal [4 + 2] acid-catalyzed aza-Diels–Alder cycloaddition with cyclic dienophiles,[19] the fused furan or pyran rings maintained the *cis* stereochemistry and the theoretically possible *trans* orientation was never detected. Hence, only the two epimers at the α-amino center, *cis* (**a**) and *trans* (**b**), were obtained as racemic mixtures (Scheme 1). The SAR study shown in the next section indicated that the *cis* (**a**) isomers always showed much higher σ_1R binding potencies than the corresponding *trans* (**b**) derivatives. In this sense, the $Mg(ClO_4)_2$-mediated protocol was also the best, since it provided *cis* diastereomers as major isomers (Table 1 shows the proportion of representative examples). In all cases *cis*/*trans* mixtures were obtained and separated by column purification or by recrystallization. The stereochemical assignment of the isolated diastereomers was established by NMR with NOE studies: the *cis* adducts in dihydropyran derivatives showed NOE effects between H_5 and H_{10b} and H_5 and H_{4a}, while the *trans* adducts showed NOEs between H_{4a} and protons of the R_2 group.

Table 1. *cis*:*trans* Ratios for Representative Pyranoquinolines

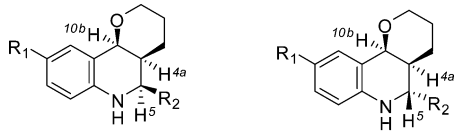

a, *rac-cis* **b**, *rac-trans*

compd	R_1	R_2	**a**:**b** ratio[a]
8	4-chlorophenoxy	cyclohexyl	78:22
9[b]	3-chlorophenoxy	cyclohexyl	83:17
17	isopentyloxy	cyclohexyl	87:13
20	phenyl	cyclohexyl	81:19
32	isopentyloxy	tetrahydro-2*H*-pyran-4-yl	90:10

[a]Diastereomeric ratio determined by ^{1}H NMR of the crude product. [b]Isolated yields: 71% (**a**) and 18% (**b**).

The synthesis of the piperidinyl-substituted pyranoquinoline analogues **34a**–**36a**, was accomplished from the Boc-protected intermediate **33a** (Scheme 2). Deprotection of **33a** with TFA provided **34a**, and subsequent reductive amination gave the alkylated derivatives **35a** and **36a**. Finally, the acetylated pyranoquinoline **37a** (Figure 2) was obtained from **17a** with Ac_2O under microwave irradiation.

The enantiomeric resolution of the most active compounds (Table 5) was undertaken by chiral HPLC. Several analytical conditions were tried, and an *n*-heptane/ethanol (98:2) mixture as the mobile phase with a Chiralpak AD-H column was found to provide the best separation of the two enantiomers. These conditions were used for enantiomeric excess (ee) determi-

Scheme 1[a]

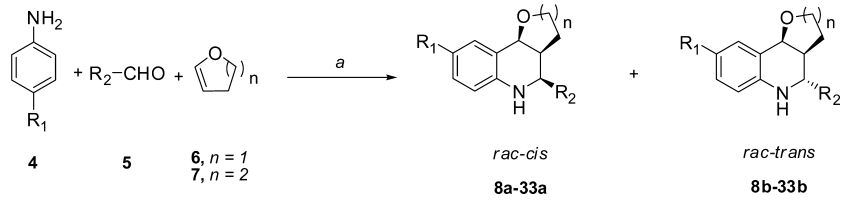

[a]Reagents and conditions: (a) $Mg(ClO_4)_2$ (5 mol %), MeCN, rt, 16 h.

dx.doi.org/10.1021/jm400181k | J. Med. Chem. 2013, 56, 3656–3665

Scheme 2[a]

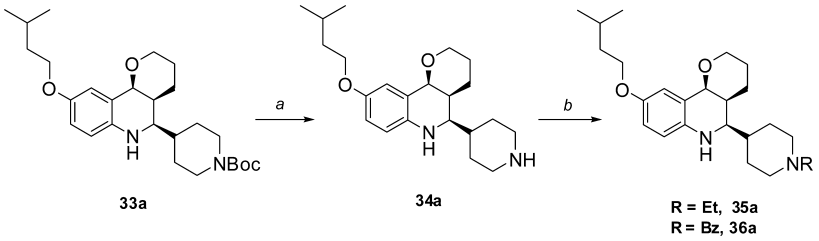

[a]Reagents and conditions: (a) DCM/TFA (5%) rt, 16 h; (b) (for **35a**) MeCHO, $NaBH_3CN$, MeOH, 90 °C, 24 h; (for **36a**) BnCHO, $NaBH(OAc)_3$, DCE, microwave, 90 °C, 10 min.

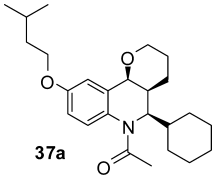

Figure 2. Structure of acetylated compound **37a**.

nation and applied to a preparative method which allowed the separation of the pairs **15c/d**, **17c/d**, and **32c/d** to give the individual enantiomers with good ee. As indicated below, only one of the enantiomers (**c**) was active, and to elucidate the absolute configuration of the eutomers, a single-crystal X-ray diffraction (SCXRD) study of the most interesting compound, **32c**, was undertaken. Since no suitable crystals were obtained using the free base, a limited salt screening was carried out. The hydrochloride provided crystals suitable for SCXRD analysis, from which the absolute configuration was reliably determined by anomalous dispersion effects (Flack −0.12(0.05)). As shown in Figure 3, the absolute configuration 4a*S*,5*R*,10b*S* was established for **32c**, confirming the *cis* stereochemistry earlier assigned.

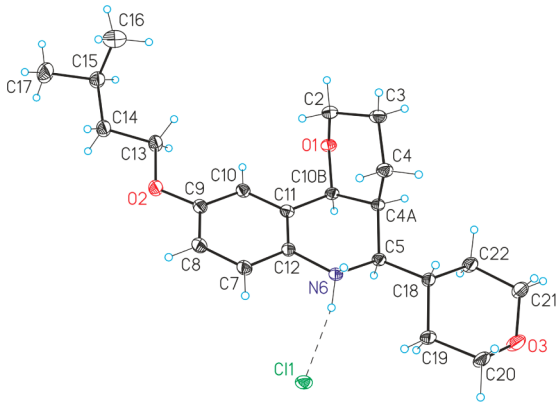

Figure 3. ORTEP plot (50%) showing the molecular structure of the hydrochloride salt of **32c**, which established the absolute configuration as 4a*S*,5*R*,10b*S*.

The preparative chiral HPLC method was scaled up for the separation of 4 g of racemic **32a** to provide **32c** with an ee > 99% in 35% yield. A diastereomeric salt resolution method was also assayed, using several chiral resolving agents: [(1*S*)-*endo*]-(+)-3-bromo-10-camphorsulfonic acid, (1*S*)-(+)-10-camphorsulfonic acid, and (*S*)-(+)-1,1′-binaphthalene-2,2′-diyl hydrogen phosphate. Enantiomerical enrichment was only achieved by crystallization with the binaphthalene derivative in acetone, which provided enantiomer **32c** as the corresponding salt. After final liberation, **32c** was isolated with an ee > 99% and an overall yield of 31%. The enantiomers of **32b** (**32e** and **32f**, Figure 4) were not separated, and both of them were assumed to be inactive in view of the inactivity of the racemic mixture.

RESULTS AND DISCUSSION

The new series was identified from an HTS campaign through an in vitro σ_1R binding assay using [^{3}H]-(+)-pentazocine[23] as the radioligand. Compound **8a**, which was part of our internal compound library and had not been previously described, emerged as a hit with submicromolar affinity for σ_1R and K_i greater than 1000 nM for σ_2R ([^{3}H]di-*o*-tolylguanidine[24] was used as the radioligand for σ_2R binding assays). This prompted the selection of **8a** for a hit to lead program, since we knew from our previous work that it is quite challenging to find high selectivity for the σ_1 versus the σ_2 receptor, while it is highly desirable on the basis of the clear-cut distinctive pharmacological functions attributed to both receptors. Another interesting feature of compound **8a** was that it did not contain a highly basic amino group, typically present in σ_1R ligands. As recently summarized by Wünsch et al.,[25] several pharmacophores reported in the literature (Figure 1B depicts Glennon's σ_1R pharmacophore) share an amine and at least two hydrophobic regions at a certain distance from the basic amino group, whose pK_a is normally above 6.5. Compound **8a** contained two hydrophobic groups at an adequate distance, but its calculated pK_a of 4.6 (ACD), was well below the usual values. The main drawback of compound **8a** was its high lipophilicity (cLogP of 7.0), which translated into a low kinetic solubility (<0.4 μM) and anticipated promiscuity and other ADMET (absorption, distribution, metabolism, excretion, toxicity) problems.[26] Thus, reduction of lipophilicity was one of the main drivers in the optimization program.

Tables 2−5 contain the binding affinities of the most relevant compounds in the series, and for the sake of comparison, the results of reference compounds **1**−**3** are included (Table 2). All the compounds showing a K_i below 1000 nM for σ_1R were tested against σ_2R, showing in all cases binding affinities superior to 1000 nM, which confirmed the good selectivity of the series.

As indicated in Table 2, there was a clear preference for the *cis* orientation, since the *trans* isomer (**8b**) of the hit was inactive, a result confirmed in the pair **9a**/**b** as well as in other examples of the series (not shown). Regarding phenoxy substitution, the 3-chloro (**9a**) and the 4-chloro (**8a**) derivatives were equipotent, while the 2-chloro (**10a**) and the unsubstituted (**12a**) analogues were devoid of activity. The 3,4-dichloro derivative **11a** showed an improved potency,

dx.doi.org/10.1021/jm400181k | J. Med. Chem. 2013, 56, 3656−3665

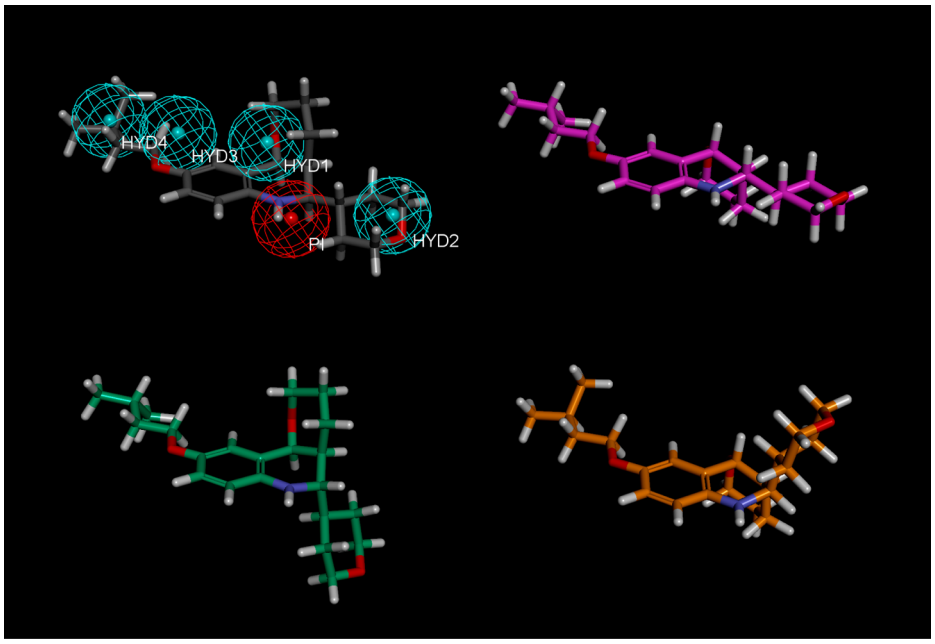

Figure 4. Minimized structures of the four accessible diastereoisomers of compound **32**. The upper left in gray shows the 4a*S*,5*R*,10b*S* diastereomer (**32c**) and its overlap with the σ_1R pharmacophore described by Laggner,[27] the upper right in pink the 4a*R*,5*S*,10b*R* diastereomer (**32d**), the lower left in green the 4a*S*,5*S*,10b*S* diastereomer (**32e**), and the lower right in orange the 4a*R*,5*R*,10b*R* diastereomer (**32f**).

Table 2. *cis*/*trans* Diastereomers of Pyranoquinolines

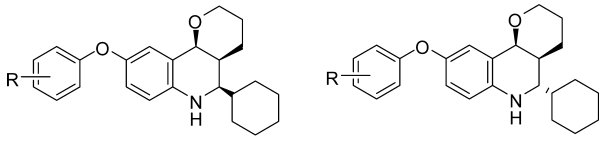

a, *rac-cis* **b**, *rac-trans*

compd	R	cLogP	$K_i(h\sigma_1)$[a] (nM)
1		3.9	17.0 ± 7.0
2		2.6	6.3 ± 1.7
3		3.8	2.1 ± 0.3
8a	4-Cl	7.0	194 ± 75
8b	4-Cl	7.0	>1000
9a	3-Cl	7.0	377 ± 81
9b	3-Cl	7.0	>1000
10a	2-Cl	6.8	>1000
11a	3,4-di-Cl	7.6	79 ± 11
12a	H	6.3	>1000

[a]Binding affinity to the human σ_1 ($h\sigma_1$) receptor in transfected HEK-293 membranes using [^{3}H]-(+)-pentazocine as the radioligand. Each value is the mean ± SD of two determinations.

Table 3. *rac-cis*-Furano- and Pyranoquinolines

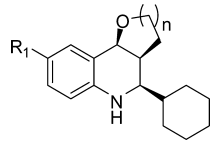

compd	R_1	*n*	cLogP	$K_i(h\sigma_1)$[a] (nM)
13a	H	2	4.2	>1000
14a	butyl	2	6.3	>1000
15a	pentyl	2	6.8	43 ± 4
16a	butoxy	2	5.9	178 ± 18
17a	isopentyloxy	2	6.3	52 ± 3
18a	(4-fluorobenzyl)oxy	2	6.2	>1000
19a	cyclohexyl	2	6.8	>1000
20a	phenyl	2	6.1	>1000
21a	(*N*-propylamino)sulfonyl	2	4.4	>1000
22a	benzamido	2	4.7	>1000
23a	(4-chlorophenyl)oxy	1	6.6	302 ± 17
24a	pentyl	1	6.4	245 ± 159
25a	butoxy	1	5.5	>1000
26a	isopentyloxy	1	5.9	108 ± 33

[a]Binding affinity to the human σ_1 ($h\sigma_1$) receptor in transfected HEK-293 membranes using [^{3}H]-(+)-pentazocine as the radioligand. Each value is the mean ± SD of two determinations.

confirming the positive effect of chlorine atoms in the 3 and 4 positions.

The R_1 group was subsequently explored over the tetrahydropyran (n = 2) or -furan (n = 1) fused frameworks, while maintaining the hit's cyclohexyl ring in R_2 (Table 3). The unsubstituted **13a** and other short-chain-substituted tetrahydropyrans of diverse electronic nature were inactive (F, OH, SMe, not shown). Interestingly enough, going from a butyl (**14a**) to a pentyl (**15a**) group resulted in a dramatic improvement in potency, suggesting that a minimum chain length of five atoms was essential for activity. Alkyl groups shorter than butyl were also prepared, but as expected, they were completely inactive (results not shown). This trend was confirmed in the alkoxy derivatives where the isopentyloxy **17a** was more potent than the butoxy **16a**, and this in turn exhibited a marked improved potency versus shorter alkoxides, which were completely devoid of activity. The (4-fluorobenzyl)oxy **18a** was inactive, in contrast with the (4-chlorophenyl)oxy present in the initial hit. Direct attachment of a ring (**19a** and **20a**) was clearly detrimental, as well as introduction of polar functions such as sulfonamido (**21a**) or benzamido (**22a**). The most active substituents found in the tetrahydropyran series were introduced in the fused tetrahydrofuran analogues **23a**–**26a**, and while the trends observed were essentially the same, it

dx.doi.org/10.1021/jm400181k | *J. Med. Chem.* 2013, 56, 3656–3665

became clear that the tetrahydropyrans were always superior to the tetrahydrofurans.

Keeping the best substituents in R_1, different groups were introduced in R_2 over the tetrahydropyran scaffold (Table 4).

Table 4. *rac-cis*-Pyranoquinolines

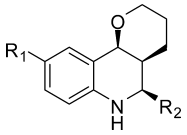

compd	R_1	R_2	cLogP	K_i ($h\sigma_1$)[a] (nM)
27a	pentyl	pentan-3-yl	6.8	410 ± 104
28a	pentyl	tetrahydro-2*H*-pyran-4-yl	4.4	67 ± 9
29a	butoxy	cyclopropyl	4.2	>1000
30a	butoxy	phenyl	4.8	>1000
31a	isopentyloxy	cyclopentyl	5.7	124 ± 5
32a	isopentyloxy	tetrahydro-2*H*-pyran-4-yl	3.9	84 ± 23
34a	isopentyloxy	piperidin-4-yl	3.9	536 ± 68
35a	isopentyloxy	1-ethylpiperidin-4-yl	4.8	317 ± 20
36a	isopentyloxy	1-benzylpiperidin-4-yl	6.1	15 ± 2

[a]Binding affinity to human σ_1 ($h\sigma_1$) receptor in transfected HEK-293 membranes using [^{3}H](+)-pentazocine as radioligand. Each value is the mean ± SD of two determinations.

Ring opening (**27a** vs **15a**), decreasing the ring size (**29a** vs **16a** and **31a** vs **17a**), and unsaturation to phenyl (**30a** vs **16a**) were detrimental for activity. On the contrary, polar atoms were tolerated in position 4 of the cyclohexyl ring: the pyranyl group (**28a**/**32a**) provided a good potency, while the unsubstituted piperidine (**34a**) showed an intermediate activity, which was improved on substitution with ethyl (**35a**) or benzyl (**36a**).

As mentioned before, in this series the pK_a of the NH (the experimental pK_a of **32c** is 3.8) is well below the usual values (pK_a above 6.5) found in σ_1 receptor ligands. The negative result of compound **37a** (Figure 2) seems to indicate that some basicity is needed, although it cannot be completely discarded that the steric bulk of the acetamide group impairs activity.

The individual *cis* enantiomers of some of the most active compounds were isolated by preparative chiral HPLC, and activity was again shown to be clearly dependent on stereochemistry, since only one enantiomer was active (Table 5). As indicated above, the absolute configuration 4a*S*,5*R*,10b*S* was established for compound **32c** on the basis of the X-ray diffraction of its hydrochloride (Figure 3). This configuration was also tentatively assigned to the eutomers **15c** and **17c** on the basis of their activity.

The fact that only one of the four accessible diastereoisomers was active indicated that the 3D distribution of the hydrophobic groups matched the spatial requirements of σ_1R, thus compensating for the lack of nitrogen basicity. The global minimum conformation of compound **32c**, which corresponds with the experimental X-ray crystal structure, was modeled into Laggner's σ_1R pharmacophore, reproduced on the basis of the reported coordinates.[27] As indicated in Figure 4, compound **32c** matched quite well the pharmacophore: the *cis*-tetrahydropyrano ring exquisitely maps the hydrophobic feature HYD1, the tetrahydropyranyl group at R_2 matches the second one (HYD2), and substitution at R_1 by the isopentyloxy group covers the two remaining hydrophobic regions (HYD3 and HYD4). The amino group matches the positive ionizable (PI)

Table 5. Enantiomers of Selected Pyranoquinolines

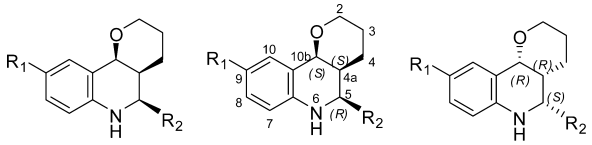

a, *rac-cis* **c**, *4aS,5R,10bS* **d**, *4aR,5S,10bR*

compd	R_1	R_2	cLogP	K_i($h\sigma_1$)[a] (nM)
15a	pentyl	cyclohexyl	6.8	43 ± 3
15c[b]	pentyl	cyclohexyl	6.8	19 ± 5
15d[b]	pentyl	cyclohexyl	6.8	>1000
17a	isopentyloxy	cyclohexyl	6.3	52 ± 3
17c[b]	isopentyloxy	cyclohexyl	6.3	14 ± 1
17d[b]	isopentyloxy	cyclohexyl	6.3	>1000
32a	isopentyloxy	tetrahydro-2*H*-pyran-4-yl	3.9	84 ± 23
32c[c]	isopentyloxy	tetrahydro-2*H*-pyran-4-yl	3.9	30 ± 8
32d[c]	isopentyloxy	tetrahydro-2*H*-pyran-4-yl	3.9	>1000

[a]Binding affinity to the human σ_1 ($h\sigma_1$) receptor in transfected HEK-293 membranes using [^{3}H]-(+)-pentazocine as the radioligand. Each value is the mean ± SD of two determinations. [b]Absolute configuration inferred from **32**. [c]Absolute configuration determined by X-ray diffraction (see Figure 3).

site of the pharmacophore, confirming thereby its function as the traditional amine site of σ_1R ligands. This explains why, even if weak, certain basicity is needed, as shown by the lack of affinity of the acetylated derivative **37a**. This model also explains that, to fit with HYD4, a minimum five-atom chain length is required in position R_1. Regarding stereospecificity, the minimum energy conformations of the remaining three diastereomers were obtained as well, after a systematic conformational search with minimization at each step. The minima thus obtained were mapped into Laggner's pharmacophore, the result being that none of them fit into the model without missing any feature. As shown in Figure 4, either one or both of HYD1 and HYD2 are not covered by the inactive diastereomers, highlighting the importance of these two hydrophobic features for the σ_1R–ligand interaction.

Some of the most active compounds (**15c**, **17c**, and **36a**) showed up to a 1 unit reduction in lipophilicity versus **8a**, but still their kinetic solubility was below 1 μM. However, compound **32c** exhibited a much more reduced lipophilicity (cLogP = 3.9) than that of **8a** (cLogP = 7.0), which translated into a solubility of 6.6 μM. The change of the 4-chlorophenyloxy group to isopentyloxy reduced the cLogP by almost 1 unit, but most relevant was the change of cyclohexyl to pyranyl, which provided an additional 2.4 unit reduction. The reduction of lipophilicity resulted in an improvement in ligand efficiency (LE; **8a**, 0.2; **32c**, 0.3), lipophilic ligand efficiency (LLE; **8a**, −0.3; **32c**, 3.6), and ligand-efficiency-dependent lipophilicity (LELP; **8a**, 35; **32c**, 12.7) indices. However, the topological polar surface area (tPSA) was maintained in the same range for the two compounds (**8a**, 30.5 Å^2; **32c**, 39.7 Å^2), predicting a good blood–brain barrier (BBB) penetration.

Compound **32c** was selected for further profiling. Additionally to its high selectivity versus σ_2R, it did not show significant affinity (inhibition at 10 μM <50%) for another 163 molecular targets (receptors, transporters, ion channels, and enzymes).[28] The only exception was the human serotonin 5-HT$_{2B}$ receptor, to which it showed a low binding affinity (K_i = 5.3 μM). This result together with that observed in **1**,[14] which only hits the 5-

dx.doi.org/10.1021/jm400181k | *J. Med. Chem.* 2013, 56, 3656–3665

HT_{2B} receptor in the same selectivity panel, suggests some structural similarity between the σ_1 and 5-HT_{2B} receptor binding sites.

In vivo evaluation of **32c** was done using a mouse model of neurogenic pain induced by intraplantar injection of capsaicin,[10] where immediate paw licking and delayed mechanical hypersensitivity are indicators of ongoing pain and pain sensitization, respectively. It inhibited mechanical hypersensitivity by 63% after oral administration at 80 mg/kg. It was also active in the formalin test, where it exerted a dose-dependent analgesic effect on phase II of formalin-induced pain (40% and 81% inhibition after intraperitoneal (ip) administration at 40 and 80 mg/kg, respectively). This antinociceptive activity was indicative of its antagonist nature, in accordance with the reported analgesic effect of σ_1R antagonists, particularly on the formalin test.[29]

Compound **32c** showed a good preliminary ADMET profile: the inhibition of cytochrome P450 was assessed in recombinant human cytochrome P450 isoforms (1A2, 2C9, 2C19, 2D6, and 3A4),[30] and the IC_{50} values were higher than 5 μM, suggesting a low potential of compound **32c** for drug−drug interactions. The intrinsic clearance found in liver microsomes[31] (human, 5.0 μL/min/mg of protein; rat, 21.7 μL/min/mg of protein; mouse, 15.1 μL/min/mg of protein) predicts a moderate to low in vivo clearance. Additionally, compound **32c** did not show in vitro cytotoxic potential in the MTT (3-(4,5-dimethylthiazol-2-yl)-2,5-diphenyltetrazolium bromide) and neutral red uptake assays when tested up to 100 μM in HepG2 cells[32] and lacked genotoxic potential in the SOS/*umu* and Ames bacterial mutation assays.[33] Finally, in the human ether-a-go-go-related gene (hERG) potassium channel[34] patch clamp assay, it showed an IC_{50} > 10 μM, which predicts a low potential for cardiac toxicity.

In summary, the synthesis and pharmacological activity of a new series of hexahydro-2*H*-pyrano[3,2-*c*]quinolines as potent and selective σ_1R ligands are reported herein. This family, which was identified in an HTS campaign, showed high selectivity versus σ_2R and did not contain the highly basic amino group usually present in other σ_1R ligands. The activity was shown to reside in only one of the four accessible diastereoisomers, which perfectly oriented the hydrophobic groups to match with the receptor, as shown by the good overlap of the eutomers with Laggner's σ_1R pharmacophore. The initial hit (**8a**) potency as well as its physicochemical properties were substantially improved in a hit to lead program that led to the identification of compound **32c**, which showed a good selectivity and ADMET profile as well as antinociceptive properties in several in vivo tests, reinforcing the notion that σ_1R antagonism could be a useful strategy for treating pain. Further profiling of compound **32c** and evolution of the series will be reported in due curse.

EXPERIMENTAL SECTION

Unless otherwise noted, all materials were obtained from commercial suppliers and used without further purification. Microwave-assisted reactions were conducted with an Explorer synthesizer from CEM. Flash chromatography was performed with a forced flow of the indicated solvent system on SDS silica gel Chromagel 60 ACC (230−400 mesh) or on a CombiFlash Companion system with Redisep Rf disposable columns. ^{1}H spectra were recorded on an Agilent UNITY 300 MHz spectrometer (fitted with a 5 mm H/F/X ATB probe) or an Agilent Mercury 400 MHz spectrometer (fitted with a 5 mm ID/PFG probe) with 2 H lock in deuterated solvents. Chemical shifts (δ) are in parts per million. Commercially available reagents and solvents (HPLC grade) were used without further purification for all the analytical tests. Analytical HPLC−MS was performed on a Waters 2795-MS ZQ system using reversed-phase XBridge C18 columns (4.6 × 50 mm, 2.5 μm), gradient 2−95% solvent B (solvent A, 10 mM ammonium bicarbonate; solvent B, acetonitrile) over 5.5 min, injection volume 10 μL, flow 2.0 mL/min. Photodiode array (PDA) spectra were recorded at 220−310 nm using a Waters 2996 PDA detector. Mass spectra were obtained over the range m/z 100−800 at a sampling rate of 0.3 scan/s using a Waters ZQ instrument. Data were integrated and reported using Water Masslynx software. All compounds display purity higher than 95% as determined by this method. Accurate mass measurements were carried out using an Agilent 6540 ultra-high-definition (UHD) accurate-mass quadrupole time-of-flight (QTOF) system and obtained by electron spray ionization (ESI) in positive mode. Chiral analytical HPLC was performed on Agilent 1100 series equipment using Daicel Chiralpak AD-H columns (4.6 × 250 mm, 5 μm). UV spectra were recorded at 208, 210, and 250 nm using an Agilent 1100 diode array detector (DAD). Chiral preparative HPLC was performed on semipreparative Agilent 1100 series equipment using a Chiralpak AD-H column (20 × 250 mm, 5 μm).

Determination of Physicochemical Properties. The topological polar surface area (tPSA) was calculated using ChemDraw Ultra 10.0.3. pK_a was calculated using ACDLABS 12.0.2 and cLogP using ChemDraw Ultra 10.0.3. Solubility was measured as kinetic solubility from the compound solution at 1% DMSO in phosphate buffer at pH 7.4 by HPLC.[35] Experimental pK_a was determined by using a pHmetric technique[36] in a Sirius Analytical GlpKa instrument.

(4a*S,5*R**,10b*S**)-9-(3-Chlorophenoxy)-5-cyclohexyl-3,4,4a,5,6,10b-hexahydro-2*H*-pyrano[3,2-*c*]quinoline Hydrochloride (9a) and (4a*S**,5*S**,10b*S**)-9-(3-Chlorophenoxy)-5-cyclohexyl-3,4,4a,5,6,10b-hexahydro-2*H*-pyrano[3,2-*c*]-quinoline Hydrochloride (9b).** To a solution of 4-(3-chlorophenoxy)aniline (220 mg, 1 mmol) in dry acetonitrile (3 mL) under an argon atmosphere were sequentially added cyclohexanecarbaldehyde (121 μL, 1 mmol) and 3,4-dihydro-2*H*-pyran (90 μL, 1 mmol), followed by $Mg(ClO_4)_2$ (12.3 mg, 0.05 mmol). The reaction mixture was stirred at room temperature for 18 h. The solvent was removed under reduced pressure and the residue taken up in CH_2Cl_2 and passed through Dicalite. The solvent was removed under reduced pressure and the crude crystallized from EtOAc to afford pure *cis* diastereomer (4a*S*,5*R**,10b*S**)-9-(3-chlorophenoxy)-5-cyclohexyl-3,4,4a,5,6,10b-hexahydro-2*H*-pyrano[3,2-*c*]quinoline (138 mg, 34%) as a white solid. The solvent from the mother liquid was evaporated and the remaining residue purified by CombiFlash chromatography (SiO_2, cyclohexane/EtOAc up to 10%) to give additional *cis* diastereomer (144 mg, overall yield 71%) along with *trans* diastereomer (4a*S*,5*S**,10b*S**)-9-(3-chlorophenoxy)-5-cyclohexyl-3,4,4a,5,6,10b-hexahydro-2*H*-pyrano[3,2-*c*]quinoline as a yellow oil (78 mg, 18%). To an ice-cooled solution of the *cis* diastereomer (50 mg, 0.13 mmol) in acetone (500 μL) was added dropwise a 2 N HCl solution in Et_2O (69 μL, 1.4 mmol). After 30 min of stirring at room temperature, a solid precipitated. The solid was filtered off and dried in vacuum to give **9a** (42 mg, 76%) as a white solid: ^{1}H NMR (400 MHz, $CDCl_3$) δ 8.12−7.93 (m, 1H), 7.26−7.22 (m, 1H), 7.21 (s, 1H), 7.10 (d, J = 7.8 Hz, 1H), 7.00 (s, 1H), 6.93 (d, J = 6.8 Hz, 1H), 6.88 (d, J = 8.3 Hz, 1H), 4.89 (d, J = 4.4 Hz, 1H), 3.62 (d, J = 10.9 Hz, 1H), 3.36−3.18 (m, 2H), 2.69−2.46 (m, 2H), 2.30−2.11 (m, 1H), 1.95−1.75 (m, 4H), 1.75−1.45 (m, 3H), 1.42−1.12 (m, 4H), 1.12−0.95 (m, 1H). The same procedure was repeated for the *trans* diastereomer to give **9b** (52 mg, 79%) as a white solid: ^{1}H NMR (400 MHz, $CDCl_3$) δ 8.11 (d, J = 7.9 Hz, 1H), 7.25 (t, J = 8.1 Hz, 1H), 7.10 (d, J = 7.9 Hz, 1H), 7.06 (d, J = 2.0 Hz, 1H), 7.02 (s, 1H), 6.92 (dd, J = 8.8, 2.2 Hz, 1H), 6.88 (dd, J = 8.4, 1.7 Hz, 1H), 4.57 (d, J = 2.5 Hz, 1H), 3.84 (dt, J = 10.3, 3.9 Hz, 1H), 3.72−3.58 (m, 2H), 2.55−2.45 (m, 1H), 2.05−1.94 (m, 2H), 1.93−1.74 (m, 6H), 1.74−1.60 (m, 2H), 1.59−1.43 (m, 2H), 1.39−1.16 (m, 3H).

(4a*R,5*S**,10b*R**)-9-(Isopentyloxy)-5-(tetrahydro-2*H*-pyran-4-yl)-3,4,4a,5,6,10b-hexahydro-2*H*-pyrano[3,2-*c*]quinoline Hydrochloride (32a).** To a solution of 4-(isopentyloxy)aniline (1.08 g,

dx.doi.org/10.1021/jm400181k | J. Med. Chem. 2013, 56, 3656−3665

6.0 mmol) in dry acetonitrile (6 mL) were sequentially added tetrahydro-2*H*-pyran-4-carbaldehyde (822 mg, 7.0 mmol), 3,4-dihydro-2*H*-pyran (668 μL, 7.0 mmol), and $Mg(ClO_4)_2$ (74.2 mg, 0.3 mmol). The reaction mixture was stirred under an argon atmosphere at room temperature for 18 h. The solvent was removed under reduced pressure and the residue taken up in CH_2Cl_2 and filtered through Dicalite. The solvent was removed under reduced pressure and the crude crystallized from EtOAc to afford pure *cis* diastereomer (4a*R**,5*S**,10b*R**)-9-(isopentyloxy)-5-(tetrahydro-2*H*-pyran-4-yl)-3,4,4a,5,6,10b-hexahydro-2*H*-pyrano[3,2-*c*]quinoline as a white solid (865 mg, 40%). To an ice-cooled solution of the previous compound (50 mg, 0.14 mmol) in acetone (5 mL) was added dropwise a 2 N HCl solution in Et_2O (76 μL, 0.15 mmol). After 30 min of stirring at room temperature, the solid formed was filtered off and dried in vacuum to give **32a** as a white solid (41 mg, 74%): ^{1}H NMR (300 MHz, DMSO) δ 7.21−6.75 (m, 3H), 4.95 (d, J = 5.35 Hz, 1H), 4.05−3.81 (m, 4H), 3.56 (d, J = 10.79 Hz, 1H), 3.40−3.04 (m, 4H), 2.25 (d, J = 12.23 Hz, 1H), 2.07−1.84 (m, 2H), 1.85−1.38 (m, 6H), 1.38−1.07 (m, 4H), 0.92 (d, J = 6.65 Hz, 6H).

Separation of the Racemic Mixtures of 15a, 17a, and 32a by Chiral HPLC. *Analytical Setting.* Analytical HPLC was performed using a Chiralpak AD-H (Daicel) column (4.6 × 250 mm, 5 μm) with *n*-heptane/ethanol (98:2, v/v) as the mobile phase at a 0.8 mL/min flow rate (diode array detector; wavelength, 210 nm for **15a**, 208 nm for **17a**, and 250 nm for **32a**; retention times, 6.7 min for **15c**, 9.4 min for **15d**, 13.6 min for **17c**, 34.9 min for **17d**, 46.2 min for **32d** (4a*R*,5*S*,10b*R*), and 66.7 min for **32c** (4a*S*,5*R*,10b*S*). These conditions were used for enantiomeric excess determination after separation, and in all cases ee was higher than 99%.

Preparative Setting. Preparative HPLC was performed using a Chiralpak AD-H (Daicel) column (20 × 250 mm, 5 μm) with *n*-heptane/ethanol (98:2, v/v) as the mobile phase at a 10 mL/min flow rate. In this way the pairs **15c**/**d**, **17c**/**d**, and **32c**/**d** were separated at the 100 mg scale. In the case of **32a** the method was scaled up to separate 4 g of the racemic mixture to provide 1.58 g of **32d** and 1.46 g of **32c**.

(4a*S*,5*R*,10b*S*)-9-(Isopentyloxy)-5-(tetrahydro-2*H*-pyran-4-yl)-3,4,4a,5,6,10b-hexahydro-2*H*-pyrano[3,2-*c*]quinoline (32c) by Diastereomeric Salt Formation. Compound **32a** (415 mg, 1.15 mmol) was suspended in acetone (6 mL), and (*S*)-(+)-1,1′-binaphthalene-2,2′-diyl hydrogen phosphate (0.20 g, 0.57 mmol) was added. The mixture was heated to reflux and stirred overnight. The suspension thus obtained was cooled to room temperature and filtered. The solid was washed with cold acetone and dried in vacuum (2−5 mmHg) at 45 °C for 4 h to give the (*S*)-(+)-1,1′-binaphthalene-2,2′-diyl hydrogen phosphate salt of **32c** (0.27 g, 33%). The previous compound was dissolved in CH_2Cl_2 (17 mL), and 1 M aqueous NaOH (17 mL) and water (17 mL) were added. The mixture was stirred for 10 min at room temperature. The organic layer was separated, and the aqueous layer was washed with CH_2Cl_2 (2 × 10 mL). The organic layers were joined and washed with 1 M aqueous NaOH (20 mL), brine (20 mL), and water, followed by filtration through cotton. The solution thus obtained was evaporated under vacuum to give the free base of **32c** as a white solid (127 mg, 93%, >99% ee).

(4a*R,5*S**,10b*R**)-9-(Isopentyloxy)-5-(piperidin-4-yl)-3,4,4a,5,6,10b-hexahydro-2*H*-pyrano[3,2-*c*]quinoline Hydrochloride (34a).** To a stirred solution of **33a**, obtained by multicomponent reaction (MCR) without further purification (400 mg, 0.87 mmol), in dry CH_2Cl_2 (5 mL), was added at 0 °C TFA (1 mL). The solution was allowed to reach room temperature and stirred under an argon atmosphere for 18 h. The reaction was then neutralized with NaOH solution and extracted with CH_2Cl_2. The combined organic fractions were washed with saturated aqueous NaCl solution, dried over Na_2SO_4, and concentrated under reduced pressure. After filtration (4a*R**,5*S**,10b*R**)-9-(isopentyloxy)-5-(piperidin-4-yl)-3,4,4a,5,6,10b-hexahydro-2*H*-pyrano[3,2-*c*]quinoline was obtained as a viscous yellow solid (270 mg, 86%). Formation of the hydrochloride in the same conditions used for the preparation of **32a** provided **34a** as a white solid (57 mg, 68%): ^{1}H NMR (300 MHz, $CDCl_3$) δ 9.80−9.58 (m, 1H), 9.58 − 9.30 (m, 1H), 6.97 (s, 1H), 6.82−6.58 (m, 2H), 4.97 (d, J = 5.36 Hz, 1H), 3.92 (t, J = 6.68 Hz, 2H), 3.81−3.66 (m, 1H), 3.66−3.51 (m, 2H), 3.39 (t, J = 11.65 Hz, 1H), 3.27−3.05 (m, 1H), 3.05−2.74 (m, 2H), 2.32−2.07 (m, 2H), 2.07−1.33 (m, 11H), 0.95 (d, J = 6.57 Hz, 6H).

(4a*S,5*R**,10b*S**)-5-(1-Ethylpiperidin-4-yl)-9-(isopentyloxy)-3,4,4a,5,6,10b-hexahydro-2*H*-pyrano[3,2-*c*]quinoline Hydrochloride (35a).** To a solution of **34a** (80 mg, 0.22 mmol) in MeOH (2.5 mL) was added acetaldehyde (31 μL, 0.55 mmol) followed by $NaBH_3CN$ (42 mg, 0.66 mmol). The reaction solution was heated at 90 °C for 24 h. After the solution was cooled to room temperature, the solvent was removed under reduced pressure. The residue was taken up in EtOAc and washed with saturated aqueous $NaHCO_3$ solution. The organic phase was dried over $MgSO_4$ and the solvent removed under reduced pressure. The residue was purified by CombiFlash chromatography (SiO_2, cyclohexane/EtOAc) to afford (4a*S**,5*R**,10b*S**)-5-(1-ethylpiperidin-4-yl)-9-(isopentyloxy)-3,4,4a,5,6,10b-hexahydro-2*H*-pyrano[3,2-*c*]quinoline (21 mg, 26%). Formation of the hydrochloride in the same conditions used for the preparation of **32a** provided **35a** as a white solid (7.5 mg, 50%): ^{1}H NMR (300 MHz, $CDCl_3$) δ 6.95 (d, J = 2.5 Hz, 1H), 6.68 (dd, J = 8.6, 2.6 Hz, 1H), 6.50 (d, J = 8.7 Hz, 1H), 5.00 (d, J = 5.4 Hz, 1H), 3.92 (t, J = 6.7 Hz, 2H), 3.75−3.51 (m, 3H), 3.42 (t, J = 11.2 Hz, 1H), 3.13 (d, J = 9.6 Hz, 1H), 3.05 (q, J = 7.2 Hz, 2H), 2.70−2.46 (m, 2H), 2.27−2.02 (m, 4H), 2.01−1.89 (m, 1H), 1.89−1.59 (m, 5H), 1.49 (t, J = 7.4 Hz, 3H), 1.56−1.40 (m, 3H), 0.95 (d, J = 6.6 Hz, 6H).

(4a*R,5*S**,10b*R**)-5-(1-Benzylpiperidin-4-yl)-9-(isopentyloxy)-3,4,4a,5,6,10b-hexahydro-2*H*-pyrano[3,2-*c*]quinoline Hydrochloride (36a).** A microwave vial was charged, under an argon atmosphere, with **39a** (80 mg, 0.22 mmol), benzaldehyde (24 mg, 0.22 mmol), and $NaBH(OAc)_3$ (95 mg, 0.44 mmol) followed by DCE (2.5 mL). The reaction mixture was heated using a microwave reactor at 90 °C for 10 min. After the mixture was cooled back to room temperature, the reaction mixture was quenched with saturated $NaHCO_3$ solution and diluted with CH_2Cl_2. The phases were separated, and the aqueous phase was extracted with CH_2Cl_2. The combined organic phases were dried over $MgSO_4$, and the solvent was removed under reduced pressure. The residue was purified by CombiFlash chromatography (SiO_2, cyclohexane/EtOAc) to afford (4a*R**,5*S**,10b*R**)-5-(1-benzylpiperidin-4-yl)-9-(isopentyloxy)-3,4,4a,5,6,10b-hexahydro-2*H*-pyrano[3,2-*c*]quinoline (38 mg, 38%). Formation of the hydrochloride in the same conditions used for the preparation of **32a** provided **36a** as a white solid (20 mg, 54%): ^{1}H NMR (300 MHz, $CDCl_3$) δ 11.21 (br s, 2H), 7.73−7.54 (m, 2H), 7.50−7.33 (m, 4H), 7.02 (s, 1H), 6.78 (d, J = 8.61 Hz, 1H), 5.02−4.86 (m, 1H), 4.56−4.36 (m, 1H), 4.37−4.16 (m, 1H), 3.94 (t, J = 6.65 Hz, 2H), 3.89−3.71 (m, 2H), 3.62 (d, J = 10.83 Hz, 1H), 3.50−3.24 (m, 3H), 3.24−3.06 (m, 1H), 3.06−2.52 (m, 3H), 2.50−2.23 (m, 2H), 2.11−1.31 (m, 8H), 0.95 (d, J = 6.56 Hz, 6H).

1-((4a*S,5*R**,10b*S**)-5-Cyclohexyl-9-(isopentyloxy)-3,4,4a,5-tetrahydro-2*H*-pyrano[3,2-*c*]quinolin-6(10b*H*)-yl)ethanone (37a).** A mixture of **17a** (100 mg, 0.28 mmol) and acetic anhydride (480 μL, 5.08 mmol) was heated using a microwave reactor at 120 °C for 20 min. After the mixture was cooled back to room temperature, the reaction mixture was quenched with H_2O and extracted with EtOAc. The combined organic fractions were dried over Na_2SO_4, and the solvent was removed under reduced pressure to give **37a** (56 mg, 51%) as an oil: ^{1}H NMR (300 MHz, $CDCl_3$) δ 7.13−6.92 (m, 2H), 6.80 (dd, J = 2.91, 8.77 Hz, 1H), 4.51 (d, J = 5.29 Hz, 1H), 4.12−3.90 (m, 3H), 3.71 (ddd, J = 3.26, 7.74, 11.00 Hz, 1H), 2.38 (p, J = 5.78 Hz, 1H), 2.07 (s, 3H), 1.95−1.44 (m, 14H), 1.31 − 0.79 (m, 5H), 0.97 (d, J = 6.56 Hz, 6H).

Single-Crystal X-ray Structure Determination of 32c. *Crystallization and Sample Preparation.* Crystals of the hydrochloride salt of **32c** were obtained by slow evaporation of an ethanol solution of the compound. The measured crystal was prepared under inert conditions immersed in perfluoropolyether as a protecting oil for manipulation.

Data Collection. Crystal structure determination for the hydrochloride salt of **32c** was carried out using an Apex DUO Kappa four-

axis goniometer equipped with an APPEX 2 4K charge-coupled device (CCD) area detector, a Microfocus Source E025 IuS using Mo Kα radiation, Quazar MX multilayer optics as the monochromator, and an Oxford Cryosystems low-temperature device, Cryostream 700 plus (T = −173 °C). Full-sphere data collection was used with ω and φ scans. Programs used: data collection, APEX-2;[37] data reduction, Bruker Saint V/.60A;[38] absorption correction, SADABS.[39]

Structure Solution and Refinement. Crystal structure solution was achieved using direct methods as implemented in SHELXTL[40] and visualized using the program XP. Missing atoms were subsequently located from difference Fourier synthesis and added to the atom list. Least-squares refinement on F^2 using all measured intensities was carried out using the program SHELXTL. All non-hydrogen atoms were refined, including anisotropic displacement parameters. The chlorine anion corresponding to one cationic molecule is distributed in two half-positions located on 2-fold rotation axes and shared with the neighboring cationic molecules.

Crystal data at 100 K: $C_{22}H_{34}Cl_1N_1O_3$, 395.95 g mol^{-1}, monoclinic, $C2$, a = 24.7260(15) Å, b = 8.9820(5) Å, c = 9.8850(6) Å, α = 90°, β = 104.524(6)°, γ = 90°, V = 2125.2(2) Å^3, Z = 4, ρ_{calcd} = 1.238 Mg/m^3, R1 = 0.0495 (0.0640), wR2 = 0.1186 (0.1273), Flack[41] −0.12(5), for 7265 reflections with $I > 2\sigma(I)$ (for 8603 reflections [R_{int} = 0.0677] with a total of 33765 measured reflections), goodness-of-fit on F^2 1.053, largest difference peak (hole) 0.842 (−0.527) e Å^{-3}.

Molecular Modeling Studies. Global mimimun energy conformations were found using the generate conformations protocol implemented in Discovery Studio 3.5[42] with a systematic search method, setting the sp^3−sp^3, sp^3−sp^2, and sp^2−sp^2 torsion increments to 60, 60, and 180, respectively, and minimizing the conformation candidates in the gas phase using the MMFF force field. As the starting conformation the crystal structure of **32c** was used, confirming it as a global minima, whereas the diastereomers were obtained by stereochemical inversion of the whole neutralized compound in the case of the enantiomer (**32d**) or by inversion of the individual stereogenic centers in the case of the *trans* disastereomers. Laggner's σ_1 pharmacophore[27] was reproduced as well in Discovery Studio 3.0 from the details on tolerance, coordinates, and distances given by the authors, and the ligand−pharmacophore mappings were done by the Catalyst program embedded in this system with a rigid fitting method.

Human σ_1 Receptor Radioligand Assay.[23] The binding properties of the test compounds to human σ_1R were studied in transfected HEK-293 membranes using [^{3}H]-(+)-pentazocine (Perkin-Elmer, NET-1056) as the radioligand. The assay was carried out with 7 μg of membrane suspension, [^{3}H]-(+)-pentazocine (5 nM) in either the absence or the presence of either buffer or 10 μM haloperidol for total and nonspecific binding, respectively. The binding buffer contained Tris−HCl (50 mM, at pH 8). The plates were incubated at 37 °C for 120 min. After the incubation period, the reaction mixture was transferred to MultiScreen HTS, FC plates (Millipore) and filtered, and the plates were washed (three times) with ice-cold Tris−HCl (10 mM, pH 7.4). The filters were dried and counted at approximately 40% efficiency in a MicroBeta scintillation counter (Perkin-Elmer) using EcoScint liquid scintillation cocktail.

Guinea Pig σ_2 Receptor Radioligand Assay. The binding properties of test compounds to guinea pig σ_2R were studied in guinea pig brain membranes as described[24] with some modifications. [^{3}H]Di-*o*-tolylguanidine (DTG) (Perkin-Elmer, code NET-986) was used as the radioligand. The assay was carried out with 200 μg of membrane suspension, [^{3}H]DTG (10 nM) in either the absence or the presence of either buffer or 10 μM haloperidol for total and nonspecific binding, respectively. The binding buffer contained Tris−HCl (50 mM, pH 8), and the σ_1 receptor was blocked with (+)-SKF10047 at 400 nM. The plates were incubated at 25 °C for 120 min. After the incubation period, the reaction mixture was transferred to MultiScreen HTS, FC plates (Millipore) and filtered, and the plates were washed three times with ice-cold 50 mM Tris−HCl (pH 7.4). The filters were dried and counted at approximately 40% efficiency in a MicroBeta scintillation counter (Perkin-Elmer) using EcoScint liquid scintillation cocktail.

In Vivo Tests. *Animals.* CD1 mice (Charles River, France) from 6 to 8 weeks old were used. Male mice were used for the formalin test and female mice for the capsaicin test. Animals had access to food and water ad libitum and were kept in controlled laboratory conditions with the temperature at 21 ± 1 °C and a light−dark cycle of 12 h (lights on at 7:00 a.m.). Experimental behavioral testing was carried out in a soundproof and air-regulated experimental room and was done blind with respect to treatment and surgical procedure. Experimental procedures and animal husbandry were conducted according to European guidelines regarding protection of animals used for experimental and other scientific purposes (Council Directive of Nov 24, 1986, 86/609/ECC) and received approval by the local Ethical Committee.

Formalin Test. A diluted formalin solution (20 μL of a 2.5% formalin solution, 0.92% formaldehyde) was injected into the midplantar surface of the right hind paw of the mouse. Formalin-induced nociceptive behavior was quantified as the time spent licking or biting the injected paw during two different periods individually recorded: the first period was recorded 0−5 min after the injection of formalin and was considered indicative of phase I formalin-evoked nociception; the second period was recorded 15−30 min after formalin injection and was considered indicative of phase II formalin-evoked nociception. The mice (n = 8−12 per group) received ip administration of a 10 mL/kg volume of vehicle 0.5% hydroxypropyl methyl cellulose (HPMC) (Sigma-Aldrich) or test compound 15 min before intraplantar (ipl) formalin injection.

Capsaicin Test. Capsaicin (8-methyl-*N*-vanillyl-6-nonamide) was purchased from Sigma-Aldrich and dissolved in 1% DMSO (vehicle) in physiological saline. Mice were habituated for 2 h in individual test compartments placed on an elevated mesh-bottomed platform with a 0.5 cm^2 grid to provide access to the ventral side of the paws and were then given an ipl capsaicin injection (1 μg in 20 μL of 1% DMSO) into the midplantar surface of the right hind paw. Fifteen minutes after ipl capsaicin injection, mechanical stimulation was applied onto the plantar surface of the hind paw using an automated testing device (dynamic plantar aesthesiometer, Ugo Basile, Italy). The device lifts a straight monofilament (0.5 mm in diameter) exerting a constant upward pressure of 0.5 g (4.90 mN) onto the plantar surface, and when the animal withdraws its hind paw, the mechanical stimulus automatically stops and the latency time is recorded. Latency was defined as the time from the onset of exposure to the filament to the cessation of the pressure when the sensor detected the paw withdrawal. Paw withdrawal latencies were measured in triplicate for each animal at 30 s intervals. A cutoff latency of 60 s was used in each trial. The mice (n = 8−12 per group) received vehicle 0.5% HPMC (Sigma-Aldrich) or test compound through the ip route in a volume of 10 mL/kg 15 min before capsaicin injection, and withdrawal latencies to mechanical stimulation were determined 15 min after capsaicin injection (30 min after the treatments). The effect of the treatments on mechanical hypersensitivity induced by capsaicin was calculated with the following equation: reduction of mechanical hypersensitivity (%) = ((LTD − LTV)/(CT − LTV)) × 100, where LTD and LTV are the latency times in drug- and vehicle-treated animals, respectively, and CT is the cutoff time (60 s).

■ ASSOCIATED CONTENT

Ⓢ Supporting Information

Analytical and characterization data for all the compounds. This material is available free of charge via the Internet at http://pubs.acs.org. CCDC 922502 contains the supplementary crystallographic data for this paper. These data can be obtained free of charge via www.ccdc.cam.ac.uk/conts/retrieving.html (or from the Cambridge Crystallographic Data Centre, 12 Union Rd., Cambridge CB21EZ, U.K. (fax (+44) 1223-336-033, e-mail deposit@ccdc.cam.ac.uk).

■ AUTHOR INFORMATION

Corresponding Author

*Phone: 0034934466000. E-mail: jldiaz@esteve.es (J.L.D.); calmansa@esteve.es (C.A.).

Notes

The authors declare no competing financial interest.

■ ACKNOWLEDGMENTS

We thank Albert Dordal, Xavier Monroy, Daniel Zamanillo, Inés Álvarez, Eva Ayet, Mª José Pretel, Sandra Yeste, Ariadna Balada, Ana Paz Martín, and Maite Ruíz for their expert contribution to in vitro, ADME/TOX, and in vivo studies, Miguel Angel Blázquez, Joan Andreu Morató, and Edmundo Ortega for their excellent technical assistance, and Carlos Pérez, Oscar Ferré, and Eduardo Villarroel for their contribution to compound management.

■ REFERENCES

(1) (a) Quirion, R.; Bowen, W. D.; Itzhak, Y.; Junien, J. L.; Musacchio, J. M.; Rothman, R. B.; Su, T. P.; Tam, S. W.; Taylor, D. P. A proposal for the classification of sigma binding sites. *Trends Pharmacol. Sci.* **1992**, *13*, 85−86. (b) Bowen, W. D. Sigma receptors: advances and new clinical potentials. *Helv. Pharm. Acta* **2000**, *74*, 211−218.

(2) (a) Hanner, M.; Moebius, F. F.; Flandorfer, A.; Knaus, H. G.; Striessnig, J.; Kempner, E.; Glossmann, H. Purification, molecular cloning, and expression of the mammalian sigma$_1$-binding site. *Proc. Natl. Acad. Sci. U.S.A.* **1996**, *93*, 8072−8077. (b) Kekuda, R.; Prasad, P. D.; Fei, Y. J.; Leibach, F. H.; Ganapathy, V. Cloning and functional expression of the human type 1 sigma Receptor (hSigmaR1). *Biochem. Biophys. Res. Commun.* **1996**, *229*, 553−558.

(3) Su, T. P.; Hayashi, T.; Maurice, T.; Buch, S.; Ruoho, A. E. The sigma-1 receptor chaperone as an inter-organelle signalling modulator. *Trends Pharmacol. Sci.* **2010**, *31*, 557−566.

(4) Monnet, F. P.; Debonnel, G.; Junien, J. L.; De Montigny, C. *N*-methyl-D-aspartate-induced neuronal activation is selectively modulated by sigma receptors. *Eur. J. Pharmacol.* **1990**, *179*, 441−445.

(5) Cheng, Z. X.; Lan, D. M.; Wu, P. Y.; Zhu, Y. H.; Dong, Y.; Ma, L.; Zheng, P. Neurosteroid dehydroepiandrosterone sulphate inhibits persistent sodium currents in rat medial prefrontal cortex via activation of sigma-1 receptors. *Exp. Neurol.* **2010**, *210*, 128−136.

(6) Chien, C. C.; Pasternak, G. W. Selective antagonism of opioid analgesia by a sigma system. *J. Pharmacol. Exp. Ther.* **1994**, *271*, 1583−1590.

(7) Kim, F. J.; Kovalyshyn, I.; Burgman, M.; Neilan, C.; Chien, C. C.; Pasternak, G. W. Sigma-1 receptor modulation of G-protein-coupled receptor signaling: potentiation of opioid transduction independent from receptor binding. *Mol. Pharmacol.* **2010**, *77*, 695−703.

(8) (a) Zamanillo, D.; Portillo-Salido, E.; Vela, J. M.; Romero, L. Sigma-1 receptor chaperone: pharmacology and therapeutic perspectives. In *Therapeutic Targets: Modulation, Inhibition, and Activation*; Botana, L. M., Loza, M., Eds.; John Wiley & Sons: Hoboken, NJ, 2012; Chapter 6, pp 225−278. (b) Maurice, T.; Su, T. P. The pharmacology of sigma-1 receptors. *Pharmacol. Ther.* **2009**, *124*, 195−206.

(9) Cendán, C. M.; Pujalte, J. M.; Portillo-Salido, E.; Montoliu, L.; Baeyens, J. M. Formalin-induced pain is reduced in sigma(1) receptor knockout mice. *Eur. J. Pharmacol.* **2005**, *511*, 73−74.

(10) Entrena, J. M.; Cobos, E. J.; Nieto, F. R.; Cendán, C. M.; Gris, G.; Del Pozo, E.; Zamanillo, D.; Baeyens, J. M. Sigma-1 receptors are essential for capsaicin-induced mechanical hypersensitivity: studies with selective sigma-1 ligands and sigma-1 knockout mice. *Pain* **2009**, *143*, 252−261.

(11) De la Puente, B.; Nadal, X.; Portillo-Salido, E.; Sánchez-Arroyos, R.; Ovalle, S.; Palacios, G.; Muro, A.; Romero, L.; Entrena, J. M.; Baeyens, J. M; López-García, J. A.; Maldonado, R.; Zamanillo, D.; Vela, J. M. Sigma-1 receptors regulate activity-induced spinal sensitization and neuropathic pain after peripheral nerve injury. *Pain* **2009**, *145*, 294−303.

(12) Drews, E.; Zimmer, A. Central sensitization needs sigma receptors. *Pain* **2009**, *145*, 269−270.

(13) Díaz, J. L.; Zamanillo, D.; Corbera, J.; Baeyens, J. M.; Maldonado, R.; Pericàs, M. A.; Vela, J. M.; Torrens, A. Selective sigma-1 receptor antagonists: emerging target for the treatment of neuropathic pain. *Cent. Nerv. Syst. Agents Med. Chem.* **2009**, *9*, 172−183.

(14) Díaz, J. L.; Cuberes, R.; Berrocal, J.; Contijoch, M.; Christmann, U.; Fernández, A.; Port, A.; Holenz, J.; Buschmann, H.; Laggner, C.; Serafini, M. T.; Burgueño, J.; Zamanillo, D.; Merlos, M.; Vela, J. M.; Almansa, C. Synthesis and biological evaluation of the 1-arylpyrazole class of σ_1 receptor antagonists: identification of 4-{2-[5-methyl-1-(naphthalen-2-yl)-1*H*-pyrazol-3-yloxy]ethyl}morpholine (S1RA, E-52862). *J. Med. Chem.* **2012**, *55*, 8211−8224.

(15) Glennon, R. A. Pharmacophore identification for sigma-1 (σ_1) receptor binding: application of the "*deconstruction−reconstruction−elaboration*" approach. *Mini-Rev. Med. Chem.* **2005**, *5*, 927−940.

(16) Marrazzo, A.; Cobos, E. J.; Parenti, C.; Arico, G.; Marrazzo, G.; Ronsisvalle, S.; Pasquinucci, L.; Prezzavento, O.; Colabufo, N. A.; Contino, M. A.; Gonzalez, L. G.; Scoto, M. G.; Ronsisvalle, G. Novel potent and selective σ ligands: evaluations of their agonist and antagonist properties. *J. Med. Chem.* **2011**, *54*, 3669−3673.

(17) (a) Xu, J.; Zeng, C.; Chu, W.; Pan, F.; Rothfuss, J. M.; Zhang, F.; Tu, Z.; Zhou, D.; Zeng, D.; Vangveravong, S.; Johnston, F.; Spitzer, D.; Chang, K. C.; Hotchkiss, R. S.; Hawkins, W. G.; Wheeler, K. T.; Mach, R. H. Identification of the PGRMC1 protein complex as the putative sigma-2 receptor binding site. *Nat. Commun.* **2011**, *2*, 380. (b) Ahmed, I. S.; Chamberlain, C.; Craven, R. J. S2R (Pgrmc1): the cytochrome-related sigma-2 receptor that regulates lipid and drug metabolism and hormone signaling. *Expert Opin. Drug Metab. Toxicol.* **2012**, *8*, 361−370.

(18) Crawford, K. W.; Bowen, W. D. Sigma-2 receptor agonists activate a novel apoptotic pathway and potentiate antineoplastic drugs in breast tumor cell lines. *Cancer Res.* **2002**, *1*, 313−322.

(19) (a) Povarov, S. L. α,β-unsaturated ethers and their analogues in reactions of diene synthesis. *Russ. Chem. Rev.* **1967**, *36*, 656−670. (b) Koutznetsov, V. V. Recent synthetic developments in a powerful imino Diels-Alder reaction (Povarov reaction): application to the synthesis of *N*-polyhtereocycles and related alkaloids. *Tetrahedron* **2009**, *65*, 2721−2750. (c) Bello, D.; Ramon, R.; Lavilla, R. Mechanistic variations of the Povarov multicomponent reaction and related processes. *Curr. Org. Chem.* **2010**, *14*, 332−356.

(20) Kamble, V. T.; Ekhe, V. R.; Joshi, N. S.; Biradar, A. V. Magnesium perchlorate: an efficient catalyst for the one-pot synthesis of pyrano- and furanoquinolines. *Synlett* **2007**, *9*, 1379−1382.

(21) Xia, M.; Lu, Y. D. Molecular iodine catalyzed imino-Diels-Alder reaction: efficient one-pot synthesis of pyrano[3,2-*c*]quinolines. *Synlett* **2005**, *15*, 2357−2361.

(22) More, S. V.; Sastry, M. N. V.; Yao, C.-F. TMSCl-catalyzed aza-Diels-Alder reaction: a simple and efficient synthesis for furano- and pyranoquinolines. *Synlett* **2006**, *9*, 1399−1403.

(23) DeHaven-Hudkins, D. L.; Fleissner, L. C.; Ford-Rice, F. Y. Characterization of the binding of [^{3}H](+)pentazocine to recognition sites in guinea pig brain. *Eur. J. Pharmacol.* **1992**, *227*, 371−378.

(24) Ronsisvalle, G.; Marrazzo, A.; Prezzavento, O.; Cagnotto, A.; Mennini, T.; Parenti, C.; Scoto, G. M. Opioid and sigma receptor studies. New developments in the design of selective sigma ligands. *Pure Appl. Chem.* **2001**, *73*, 1499−1509.

(25) (a) Rack, E.; Fröhlich, R.; Schepmann, D.; Wünsch, B. Design, synthesis and pharmacological evaluation of spirocyclic σ_1 receptor ligands with exocyclic amino moiety (increased distance 1). *Bioorg. Med. Chem.* **2011**, *19*, 3141−3151. (b) Glennon, R. A.; Ablordeppey, S. A.; Ismaiel, A. M.; El-Ashmawy, M. B.; Fischer, J. B.; Howie, K. B. Structural features important for σ_1 receptor binding. *J. Med. Chem.* **1994**, *37*, 1214−1219. (c) Wünsch, B. Pharmacophore models and development of spirocyclic ligands for σ_1 receptors. *Curr. Pharm. Des.* **2012**, *18*, 930−937.

(26) Leeson, P. D.; Springthorpe, B. The influence of drug-like concepts on decision-making in medicinal chemistry. *Nat. Rev. Drug Discovery* **2007**, 881−890.

(27) Laggner, C.; Schieferer, C.; Fiechtner, B.; Poles, G.; Hoffmann, R. D.; Glossmann, H.; Langer, T.; Moebius, E. F. Discovery of high-affinity ligands of σ_1 receptor, ERG2, and emopamil binding protein by pharmacophore modeling and virtual screening. *J. Med. Chem.* **2005**, *48*, 4754−4764.
(28) Selectivity panel identical to that used for characterization of compound **1** as indicated in the following paper: Romero, L.; Zamanillo, D.; Nadal, X.; Sánchez-Arroyos, R.; Rivera-Arconada, I.; Dordal, A.; Montero, A.; Muro, A.; Bura, A.; Segalés, C.; Laloya, M.; Hernández, E.; Portillo-Salido, E.; Escriche, M.; Codony, X.; Encina, G.; Burgueño, J.; Merlos, M.; Baeyens, J. M.; Giraldo, J.; López-García, J. A.; Maldonado, R.; Plata-Salamán, C. R.; Vela, J. M. Pharmacological properties of S1RA, a new sigma-1 receptor antagonist that inhibits neuropathic pain and activity-induced spinal sensitization. *Br. J. Pharmacol.* **2012**, *166*, 2289−2306.
(29) Kim, H. W.; Kwon, Y. B.; Roh, D. H.; Yoon, S. Y.; Han, H. J.; Kim, K. W.; Beitz, A. J.; Lee, J. H. Intrathecal treatment with sigma1 receptor antagonists reduces formalin-induced phosphorylation of NMDA receptor subunit 1 and the second phase of formalin test in mice. *Br. J. Pharmacol.* **2006**, *148*, 490−498.
(30) (a) Stresser, D. M. High-throughput screening of human cytochrome P450 inhibitors using fluorometric substrates. Methodology for 25 enzyme/substrate pairs. In *Optimization in Drug Discovery: In Vitro Methods*; Yan, Z., Caldwell, G. W., Eds.; Humana Press: Totowa, NJ, 2004; pp 215−230. (b) Yan, Z.; Caldwell, G. W. Evaluation of cytochrome P450 inhibition in human liver microsomes. In *Optimization in Drug Discovery: In Vitro Methods*; Yan, Z., Caldwell, G. W., Eds.; Humana Press: Totowa, NJ, 2004; pp 231−244. (c) *Drug Interaction Studies—Study Design, Data Analysis, Implications for Dosing and Labeling*; Center for Drug Evaluation and Research (CDER), Food and Drug Administration: Silver Spring, MD, September 2006 and February 2012.
(31) (a) Obach, R. S.; Baxter, J. G.; Liston, T. E.; Silber, B. M.; Jones, B. C.; MacIntyre, F.; Rance, D. J.; Wastall, P. The prediction of human pharmacokinetic parameters from preclinical and in vitro metabolism data. *J. Pharmacol. Exp. Ther.* **1997**, *283*, 46−58. (b) Obach, R. S. Prediction of human clearance of twenty-nine drugs from hepatic microsomal intrinsic clearance data: an examination of in vitro half-life approach and nonspecific binding to microsomes. *Am. Soc. Pharmacol. Exp. Ther.* **1999**, *27*, 1350−1359.
(32) Putman, K. P. Evaluation of eight in vitro assays for assessing the cytotoxicity of cigarette smoke condensate. *Toxicol. Vitro* **2000**, *16*, 599−607.
(33) (a) Maron, D. M.; Ames, B. N. Revised methods for the Salmonella mutagenicity test. *Mutat. Res.* **1983**, *113*, 173−215. (b) Reifferscheid, G.; Heil, J. Validation of the SOS/umu test using test results of 486 chemicals and comparison with the Ames test and carcinogenicity data. *Mutat. Res.* **1996**, *369*, 129−145.
(34) Diaz, G. J.; Daniell, K.; Leitza, S. T.; Martin, R. L.; Su, Z.; McDermott, J. S.; Cox, B. F.; Gintant, G. A. The [^{3}H]-dofetilide binding assay is a predictive screening tool for hERG blockade and proarrhythmia: comparison of intact cell and membrane preparations and effects of altering $[K^+]_o$. *J. Pharmacol. Toxicol. Methods* **2004**, *50*, 187−199.
(35) Sugano, K.; Okazaki, A.; Sugimoto, S.; Tavornvipas, S.; Omura, A.; Mano, T. Solubility and dissolution profile assessment in drug discovery. *Drug Metab. Pharmacokinet.* **2007**, *22* (4), 225−254.
(36) Box, K. J.; Comer, E. A. Using measured pKa, logP and solubility to investigate supersaturation and predict BCS class. *Curr. Drug Metab.* **2008**, *9*, 869−878.
(37) Data collection with APEX II versions v2009.1-02, Bruker AXS Inc., Madison, WI, 2007.
(38) Data reduction with Bruker SAINT V7.60A, Bruker AXS Inc., Madison, WI, 2007.
(39) SADABS, V2008/1, Bruker AXS Inc., Madison, WI, 2001. Blessing, R. H. An empirical correction for absorption anisotropy. *Acta Crystallogr.* **1995**, *A51*, 33−38.
(40) Sheldrick, G. M. A short history of *SHELX*. *Acta Crystallogr.* **2008**, *A64*, 112−122. (SHELXTL versions V6.12 and 6.14).
(41) Flack, H. D. On enantiomorph-polarity estimation. *Acta Crystallogr.* **1983**, *A39*, 876−881.
(42) *Discovery Studio Modeling Environment*, release 3.5; Accelrys Software Inc.: San Diego, 2012.